JTTEE5 9:107-113

Structure and Phases in Nickel-Base Self-Fluxing Alloy Coating Containing High Chromium and Boron

F. Otsubo, H. Era, and K. Kishitake

(Submitted 7 November 1998; in revised form 19 May 1999)

The structure of a nickel-base, self-fluxing alloy coating, containing chromium and boron thermal sprayed and fused, was investigated by x-ray diffraction (XRD), scanning electron microscopy (SEM), electron probe microanalysis (EPMA), and transmission electron microscopy (TEM). A lumpy M_6C carbide, a rodlike M_3B_2 boride of tetragonal structure, a rodlike M_7C_3 carbide of hexagonal structure, and a Ni-Ni_3B eutectic phase formed in the coating after fusing. Metals of M_6C, M_3B_2, and M_7C_3 phases are composed of chromium, molybdenum, and nickel; chromium and molybdenum; and mainly chromium, respectively. The nickel phase in the coating has the $L1_2$ type superlattice structure.

Keywords metallography, nickel-base self-fluxing alloy, transmission electron microscopy

1. Introduction

Nickel-base self-fluxing alloys for thermal spraying contain nickel, chromium, boron, and silicon. Chromium and boron are effective in increasing the hardness. Boron and silicon depress the melting temperature and enhance wettability by combining with oxides. The coatings have no pores and adhere well to the substrate after the fusing process and are used widely for components requiring wear and corrosion resistance.

Although the mechanical[1–7] and chemical[2,7–9] properties of nickel-base self-fluxing alloy coatings are well known, the constituents of the metallographic structure have not been fully analyzed. Bell[10] reported at first that the constituents of the coating were carbides, chromium borides, a solid solution, and a eutectic phase. After that, it was reported that (chromium, molybdenum) carbide and (chromium, molybdenum) boride,[2] Ni_3B and chromium carbides,[4] and chromium carbide and chromium boride[11,12] were present in the nickel matrix of the coating. In these works, the phases in the coating were determined from the results of composition analyses by electron probe microanalysis (EPMA), but the species of the carbides and borides were not identified.

Spridonov *et al.*[13] and Panin *et al.*[14] examined the structure and phases in the coatings metallographically and crystallographically. Spridonov reported that nickel, Cr_7C_3, CrB, Ni_3B, and Ni_5Si_2 phases were in a coating remelted by a gas torch or a laser beam. Panin indicated that the as-sprayed coating was composed of a face-centered cubic nickel solid solution containing chromium, carbon, Ni_3B, CrN, CrB, Fe_3Al, and SiO_2.

Thus, the identification of the constituents appearing in nickel-base self-fluxing alloy coatings is not sufficient, and, as well, there is no correspondence between the constituents and the microstructure of the coatings.

In this study, the structure of the nickel-base self-fluxing alloy coating after fusing was investigated by scanning electron microscopy (SEM), EPMA, transmission electron microscopy (TEM), and x-ray diffractometry (XRD). The constituents revealed in the coating were all identified and related to the microstructure.

2. Experimental Procedure

Nickel-base, self-fluxing alloys are classified by the hardness depending on the quantity of chromium and boron. A self-fluxing alloy of high chromium and boron content was investigated in this study. The alloy corresponds to JIS-MSFNi4, as shown in Table 1.[15] The alloy powder was sprayed onto a mild steel plate by means of a 40 kW plasma spraying apparatus under the conditions of 600 A, 26 V, and 100 mm spray distance. The coating thickness was about 500 μm. Subsequently, the coating was heat treated at 1323 K for 300 s in air for fusing. Some specimens were heat treated at 1323 K for 18 ks to create a coarse structure.

The specimen for TEM was prepared by means of an ion milling method at 5 kV at a tilting angle of 10° for the argon ion dual beam. Phases revealed in the coating were also examined by electron beam diffraction.

3. Results and Discussion

3.1 Structure and Constituents in Coating

Figure 1 shows backscattered electron (BSE) images of the alloy coating. It can be seen from Fig. 1(a) that a fine structure without pores forms in the as-sprayed condition. Rodlike crystals of dark image and a bright image matrix are observed after fusing, as shown in Fig. 1(b). Fig. 2 shows the BSE and SEM images of the same area of the coating, which was heat treated at 1323 K for 18 ks to coarsen the structure. There are two types of rodlike crystals of dark and gray images in addition to lumpy crystals of

F. Otsubo, H. Era, and **K. Kishitake,** Department of Materials Science and Engineering, Faculty of Engineering, Kyushu Institute of Technology, Kita-Kyushu 804-8550, Japan.

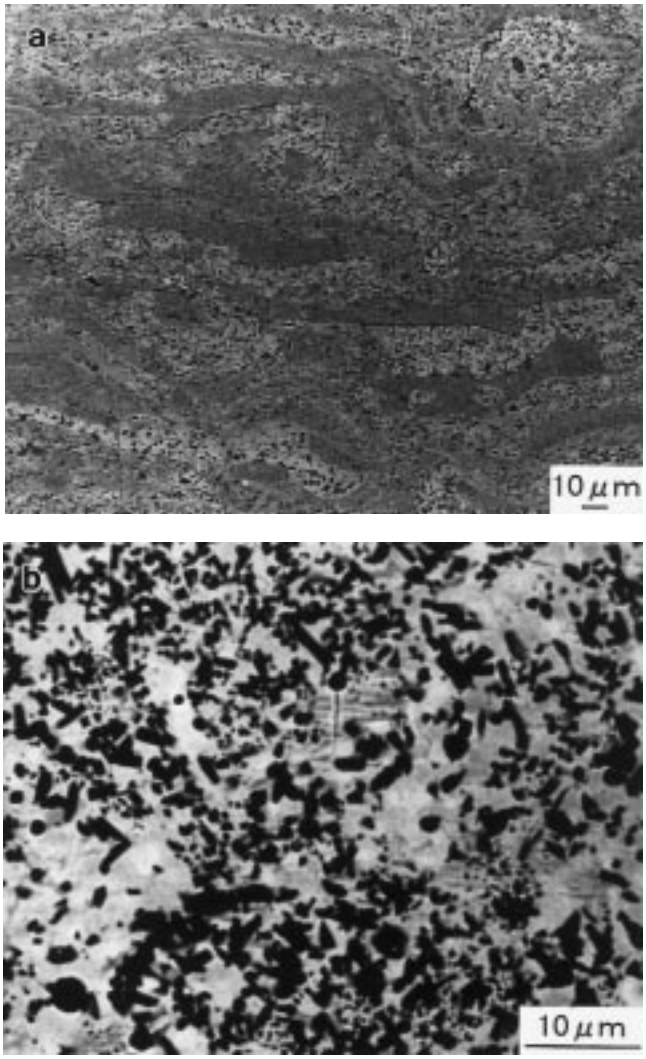

Fig. 1 BSE images of coating: (**a**) as-sprayed and (**b**) after fusing.

Table 1 Chemical composition of powder (mass%)

Element	Composition, wt.%
Ni	Bal
Cr	16.6
B	3.9
C	0.6
Si	4.1
Fe	2.4
Mo	4.0

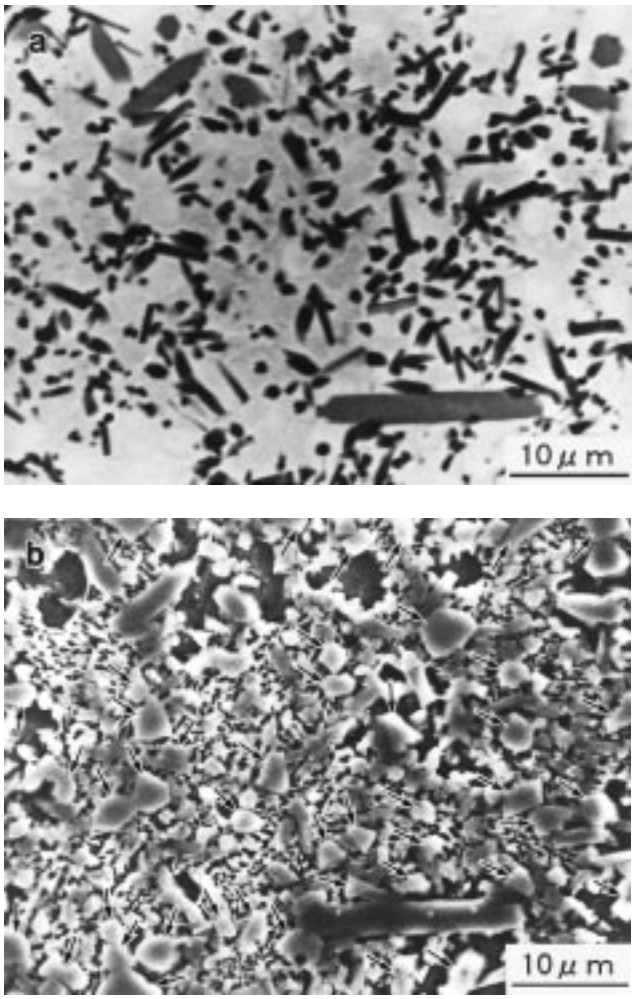

Fig. 2 Microstructure of coating heat treated at 1323 K for 18 ks: (**a**) BSE and (**b**) SEM image of same area as (**a**) after deep etching.

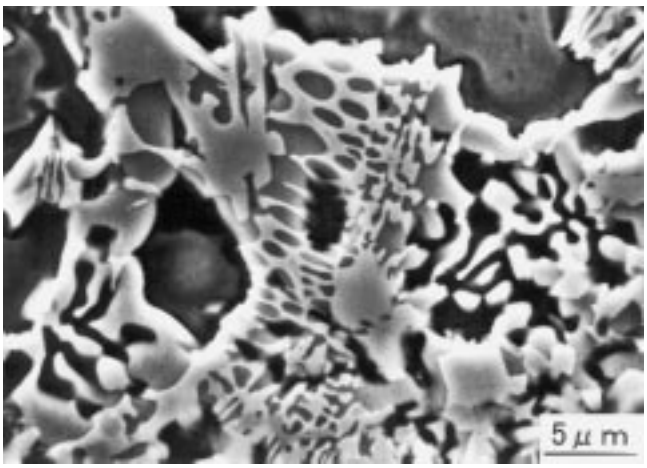

Fig. 3 SEM image of caoting heat treated at 1323 K for 18 ks.

light image (Fig. 2a). It is difficult to distinguish the lumpy crystals from the matrix in the BSE image because the contrast of the crystals to the matrix is diffuse. To better demark the lumpy crystals, the same area was deeply etched by aqua regia and observed using SEM. The lumpy crystals are clearly seen as indicated by arrows in the SEM image (Fig. 2b). Figure 3 shows a SEM image of the matrix after a light etch. It is also clear from Figure 3 that the matrix exhibits eutectic structure. This eutectic is considered to be Ni-Ni_3B eutectic from the nickel-boron phase diagram.[16] Thus, the coating structure after fusion is composed of lumpy crystals, two types of rodlike crystals, and Ni-Ni_3B eutectic.

3.2 Lumpy Crystal

Line analysis by EPMA was performed to examine the elements contained in the lumpy crystal. Figure 4 shows that the lumpy crystal contains molybdenum, chromium, nickel, and carbon, but no boron, suggesting that the lumpy crystal is a carbide containing the transition metals. Figure 5(a) shows a bright-field image of a lumpy crystal by TEM observation. Figure 5(b) shows a selected area diffraction pattern of the lumpy crystal. The diffraction pattern indicates that the crystal has a cubic structure with a lattice constant of approximately 1.08 nm. It is clear from the results of EPMA and TEM analyses that the lumpy crystal is of M_6C carbide, where M contains molybdenum, chromium, and nickel.

3.3 Rodlike Crystals

Figure 6 shows the x-ray intensity profiles obtained by EPMA for two types of rodlike crystals. Figure 6(a) and (b) correspond to the rodlike crystals of dark and gray contrast, respectively, in the BSE image shown in Figure 2(a). It is shown that the crystal of dark contrast has chromium, molybdenum, and boron, while the other crystal of gray contrast contains mainly chromium and carbon with minute amounts of molybdenum and nickel. Therefore, the crystal of dark image corresponds to a chromium boride containing molybdenum, and the other crystal of gray contrast is a chromium carbide.

Transmission electron microscopy observation was carried out to distinguish further detail. Figure 7 shows a bright-field image and the diffraction patterns obtained from the coating. The microstructure consists of three types of crystals labeled "b" through "d." The diffraction pattern shown in Fig. 7(b) was obtained from the crystal labeled b in Fig. 7(a). It was found that the crystal labeled "b" is of Ni_3B with an orthorhombic structure (a = 0.53, b = 0.66, and c = 0.44 nm). The region labeled "d" is a nickel solid solution with an ordered structure (a = 0.35 nm), which is described in the following section. The diffraction pattern shown in Fig. 7(c) was taken from the rodlike crystal labeled "c" in Fig. 7(a). It is clear from analysis of the diffraction pattern that the crystal is of M_3B_2 boride with a tetragonal structure (a = 0.58 and b = 0.31 nm), corresponding to the rodlike crystal with dark contrast in the BSE (Fig. 2a) image. The chromium carbide (Fig. 6b) is regarded to be M_7C_3 or $M_{23}C_6$ because the ratio of metal to carbon fraction in the carbide is relatively large compared with that of metal to boron fraction in the M_3B_2, as ex-

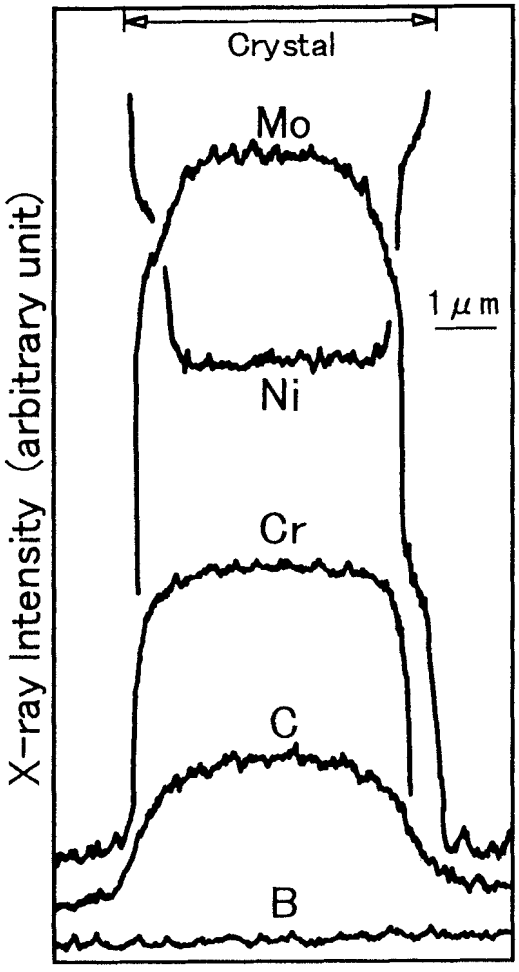

Fig. 4 X-ray intensity profiles across a lumpy crystal.

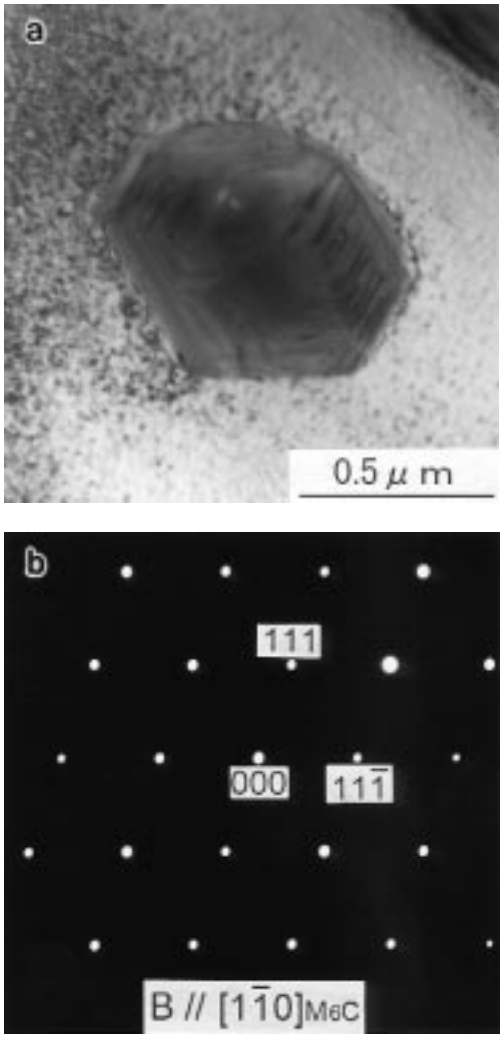

Fig. 5 TEM image of a lumpy crystal in coating: (**a**) bright-field image and (**b**) diffraction pattern.

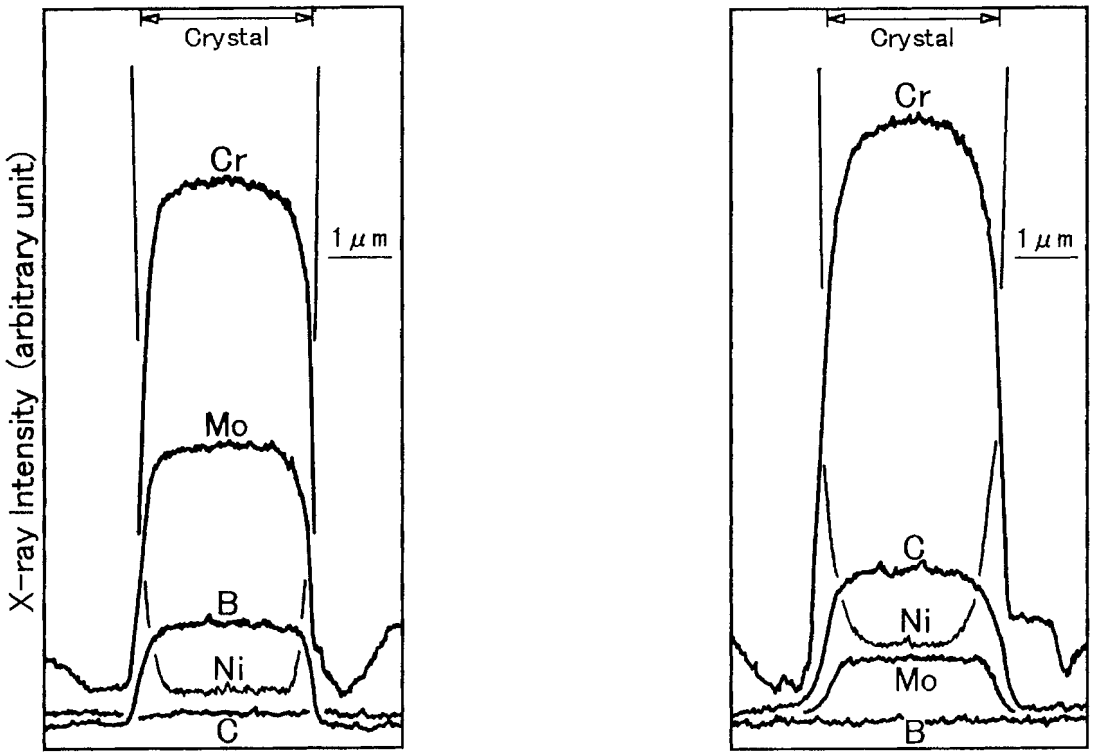

Fig. 6 X-ray intensity profiles across two kinds of rod like crystals: (**a**) dark image in Fig. 2(**a**) and (**b**) gray image in Fig. 2 (**a**).

pected from the image contrast of BSE (Fig. 2a). Figure 8(a) shows a bright-field image of the rodlike crystal, which is viewed along the longitudinal direction of the crystal. A selected area diffraction pattern of the crystal exhibits a sixfold symmetry (Fig. 8b and c), indicating that the crystal is of a hexagonal structure with a lattice constant of a = 1.41 nm. It is apparent from the trace analysis that the habit planes are parallel to $\{10\bar{1}0\}$; the crystal is surrounded by the six habit planes. From these results, it is concluded that the rodlike crystal of the gray image in the BSE (Fig. 2a) image is of M_7C_3 carbide, which consists mainly of chromium and a small amount of nickel and molybdenum (Fig. 6b). Thus, the coating is composed of M_6C, M_3B_2, and M_7C_3 in addition to nickel and Ni_3B phases as a eutectic.

3.4 Nickel Phase

The nickel phase in the alloy is of eutectic, as shown in Fig. 7(a), by the label of "d." It is seen that the diffraction patterns of the nickel phase taken from the coating exhibit weak spots in addition to the fundamental spots. The fundamental spots correspond to a disordered nickel solid solution with an A1 type structure. The weak spots are extra reflections from an ordered structure with the $L1_2$ lattice. It was found by energy dispersive x-ray analysis that the nickel phase of the coating has an atomic ratio of Ni : Fe : Cr : Si = 76 : 11 : 6 : 7, where the atomic ratio of Ni to X is 3 to 1 (X = iron, chromium, and silicon). Therefore, the nickel and X atoms (X = iron, chromium, and silicon) may occupy the sites of copper and gold atoms, respectively, in the ordered Cu_3Au prototype. Fig. 9 shows a dark-field image of the nickel phase obtained by (110) reflection of the $L1_2$ phase in the coating. It is seen that the fine spheroidal precipitates of the $L1_2$ type structure are dispersed and coherent with the matrix of the nickel solid solution. It was found that the nickel phase in the coating is accompanied with a fine dispersion of $L1_2$ phase precipitates.

As mentioned previously, the structure of the coating consists of several phases. To confirm the revealed constituents, an XRD pattern taken from the coating is shown in Fig. 10. All peaks revealed in the XRD correspond to nickel, Ni_3B, M_6C, M_3B_2, and M_7C_3 phases. Table 2 summarizes the lattice constants of the revealed phases, which are determined from the peak position. The Ni_3B phase crystallizes as a eutectic with the nickel solid solution, and the lattice constants are consistent with those reported by Shapiro and Ford.[17] Kuzma *et al.*[18] reported that $(Mo, Cr)_3B_2$ boride with a tetragonal structure forms in the Mo-Cr-B ternary system, where the boride has a composition of 29 to 40 at.% Mo, 31 to 20 at.% Cr, and 40 at.% B and the lattice constants of a = 0.583 to 0.577 nm and c = 0.312 to 0.308 nm. The M_3B_2 phase appears even in the nickel-base self-fluxing alloy coating, and the boride has a relatively lower value in the range of the previously mentioned lattice constants. The authors reported that M_3B_2 boride forms and is accompanied with $M_{23}B_6$ in an iron-base alloy with a composition of 10 wt.% Cr, 10 wt.% Mo, and 3.4 wt.% B.[19]. With increasing carbon and decreasing boron in the iron-base alloy containing carbon and boron, the M_3B_2 boride diminishes and M_6C carbide becomes predominant, coexisting with the $M_{23}B_6$ or $M_{23}C_6$ type phase. Thus, the M_3B_2 and M_6C

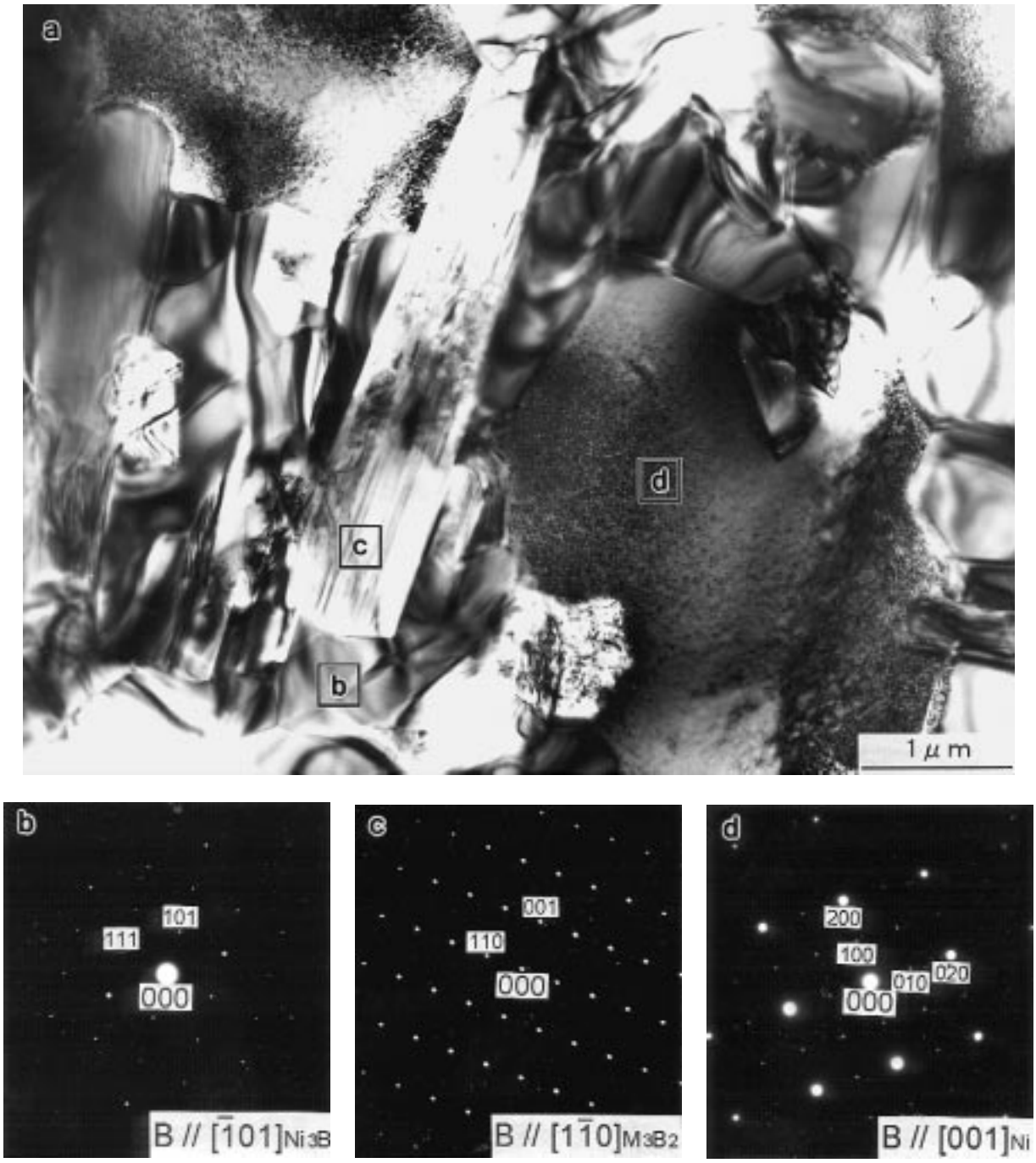

Fig. 7 TEM images of coating: (**a**) bright-field image, (**b**) diffraction pattern of crystal indicated by b in Fig.7(**a**), (**c**) diffraction pattern of rodlike crystal indicated by c in Fig. 7 (**a**), and (**d**) diffraction pattern of crystal indicated by d in Fig. 7(**a**).

type phases appear together in the iron-base alloy containing chromium, molybdenum, carbon, and boron. Formation of the boride of M_3B_2 and the carbide of M_6C in the nickel-base alloy coating is similar to that in the iron-base alloy, although the $M_{23}(C, B)_6$ is not present. The M_7C_3 carbide, in turn, appears in the nickel-base, self-fluxing alloy coating. This can be attributed to the higher content of chromium in the coating rather than the iron-base alloy.

4. Conclusions

The structure and phases in commercial nickel-base, self-fluxing alloy coating (JIS-MSFNi4) after fusing were investigated in detail by means of SEM, EPMA, XRD, and TEM. The results are summarized as follows.

- Lumpy crystals and two types of rodlike crystals in addition to the Ni-Ni_3B eutectic phase form in JIS-MSFNi4 alloy coating.

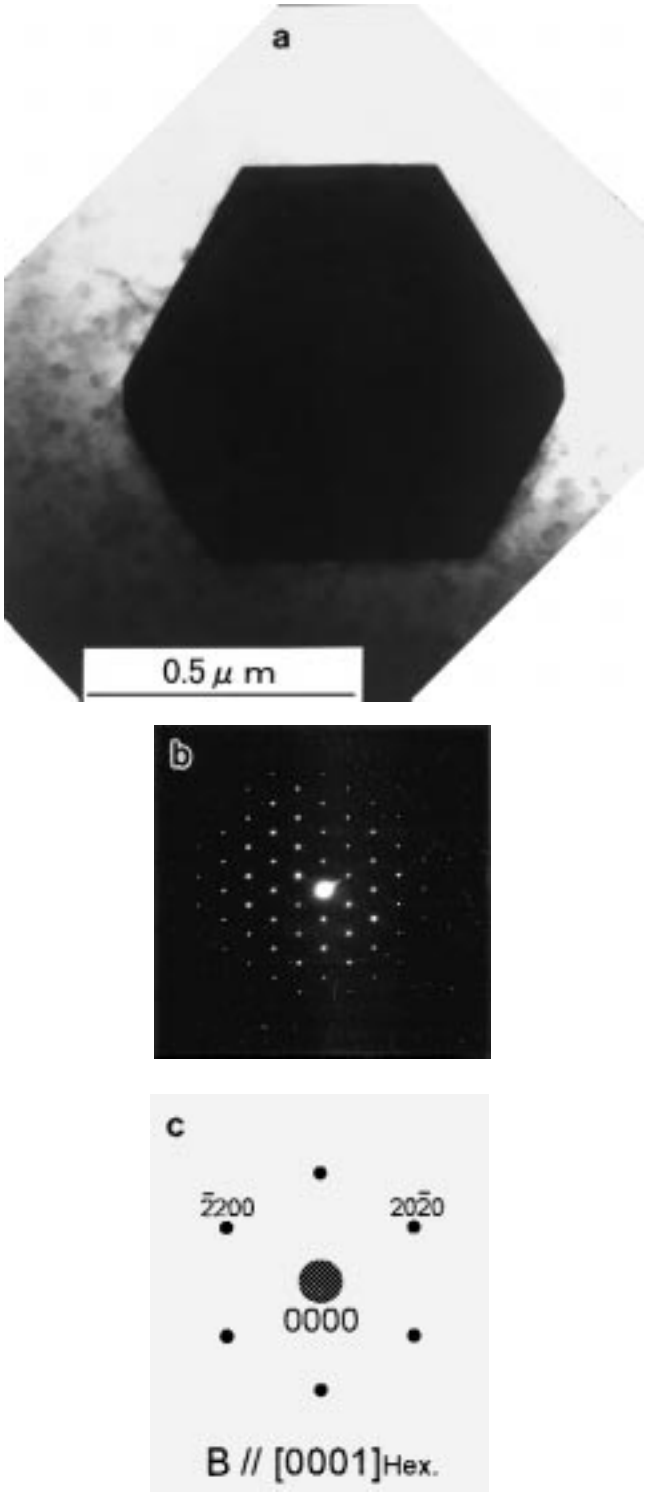

Fig. 8 TEM images of coating: (**a**) bright-field image, (**b**) diffraction pattern, and (**c**) indexed results.

- The lumpy crystal is of M_6C carbide containing chromium, molybdenum, and nickel.
- Two types of rodlike crystals correspond to M_3B_2 boride of tetragonal structure with chromium and molybdenum and M_7C_3 carbide of hexagonal structure with a large amount of chromium.
- Extremely fine spheroidal precipitates of $L1_2$ structure are extensively dispersed in a nickel phase of solid solution in the MSFNi4 alloy coating.

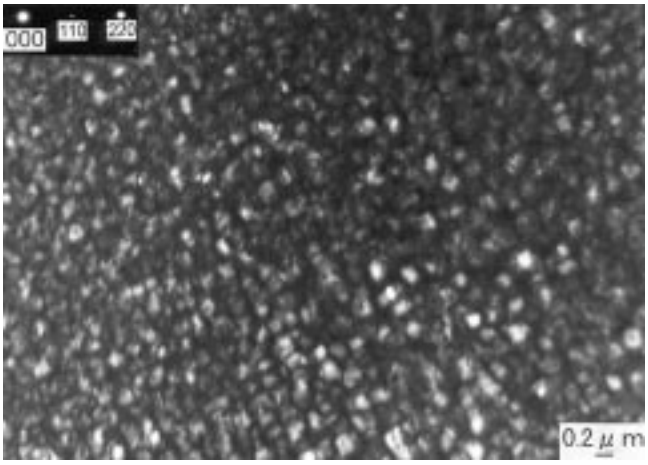

Fig. 9 Dark-field image obtained by (110) reflection of Ll_2 phase in coating.

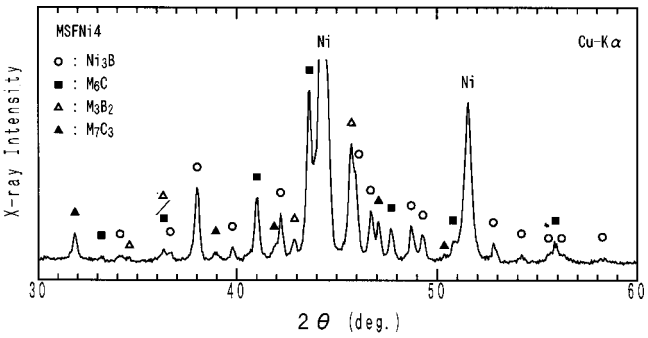

Fig. 10 XRD pattern of coating after fusing.

Table 2 Phases revealed in coating

Phase	Structure	Lattice constant, nm
Nickel (SS plus Ll_2)	Cubic	a = 0.354
Ni_3B	Orthorhombic	a = 0.528
. . .	. . .	b = 0.662
. . .	. . .	c = 0.439
M_6C	Cubic	a = 1.077
M_3B_2	Tetragonal	a = 0.578
. . .	. . .	c = 0.309
M_7C_3	Hexagonal	a = 1.413
. . .	. . .	c = 0.460

Acknowledgments

The authors wish to acknowledge the Center for Instrumental Analysis, Kyushu Institute of Technology, for EPMA measurements, TEM observation, and XRD analysis. They would also like to extend thanks to Mr. H. Ohhara for assistance.

References

1. T. Naiki and H. Anzai: *J. Jpn. Weld. Soc.*, 1959, vol. 28, pp. 295-300 (in Japanese).
2. M. Toyota, K. Usuki, S. Iwanaga, and K. Shoji: *J. Jpn. Thermal Spraying Soc.*, 1969, vol. 6, pp. 283-90 (in Japanese).
3. A. Hasui and S. Kitahara: *J. Jpn. Thermal Spraying Soc.*, 1969, vol. 6, pp. 324-39 (in Japanese).
4. N. Asahi and T. Tamamura: *J. Jpn. Thermal Spraying Soc.*, 1973, vol. 10, pp. 71-75 (in Japanese).
5. Y. Mima, M. Magome, H. Nakahira, and T. Morishita: *J. Jpn. Thermal Spraying Soc.*, 1976, vol. 13, pp. 342-48 (in Japanese).
6. Y. Shieh, J. Wang, H. Shin, and S. Wu: *Surf. Coat. Technol.*, 1993, vol. 58, pp. 73-77.
7. K. Hidaka: *Kinzoku*, Autumn, 1978, pp. 68-73 (in Japanese).
8. M. Tagaya, H. Asamura, and H. Yamanaka: *J. Jpn. Thermal Spraying Soc.*, 1964, vol. 1, pp. 6-13 (in Japanese).
9. B. Tsujino, J. Morimoto, and S. Miyase: *J. Jpn. Thermal Spraying Soc.*, 1981, vol. 18, pp. 1-6 (in Japanese).
10. G.R. Bell: *Corr. Technol.*, 1961, Mar., pp. 65-70.
11. Y. Shimagaya, G. Nakazawa, and M. Iwamoto: *J. Jpn. Thermal Sraying Soc.*, 1966, vol. 3, pp. 96-101 (in Japanese).
12. Y. Shimagaya and M. Endoh: *J. Jpn. Thermal Spraying Soc.*, 1967, vol. 4, pp. 166-73 (in Japanese).
13. N. Spiridonov, T. Opekunova, and A. Pankov: *Phys. Chem. Mater. Treatment*, 1989, vol. 23, pp. 325-30.
14. V. Panin, V. Klimenov, V. Bezborodov, and O. Perevalova: *Phys. Chem. Mater. Treatment*, 1993, vol. 27, pp. 183-87.
15. "Spray Fused Coatings of Self-Fluxing Alloys," H 8303, *Japanese Industrial Standards (JIS)*, 1994 (in Japanese).
16. T.B. Massalski: *Binary Alloy Phase Diagrams*, ASM INTERNATIONAL, Metals Park, OH, 1986, vol. 1, pp. 370.
17. S. Shapiro and J.A. Ford: *Trans. AIME*, 1966, vol. 236, pp. 536-42.
18. Yu.B. Kuzma, V.S. Telegus, and D.A. Kovalyk: *Poroshk. Metall.*, 1969, vol. 77 (5), pp. 79-87 (in Russian).
19. K. Kishitake, H. Era, F. Otsubo, and T. Hasegawa: *J. Jpn. Foundrymen's Soc.*, 1995, vol. 67, pp. 613-18 (in Japanese).